NASA/TM—2012–215972

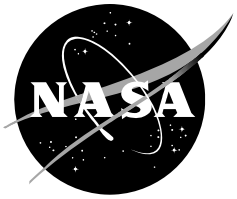

Design of Low Complexity Model Reference Adaptive Controllers

Curt Hanson and Jacob Schaefer
Dryden Flight Research Center, Edwards, California

Marcus Johnson and Nhan Nguyen
NASA Ames Research Center, Mountain View, California

May 2012

NASA STI Program ... in Profile

Since its founding, NASA has been dedicated to the advancement of aeronautics and space science. The NASA scientific and technical information (STI) program plays a key part in helping NASA maintain this important role.

The NASA STI program operates under the auspices of the Agency Chief Information Officer. It collects, organizes, provides for archiving, and disseminates NASA's STI. The NASA STI program provides access to the NASA Aeronautics and Space Database and its public interface, the NASA Technical Reports Server, thus providing one of the largest collections of aeronautical and space science STI in the world. Results are published in both non-NASA channels and by NASA in the NASA STI Report Series, which includes the following report types:

- TECHNICAL PUBLICATION. Reports of completed research or a major significant phase of research that present the results of NASA Programs and include extensive data or theoretical analysis. Includes compilations of significant scientific and technical data and information deemed to be of continuing reference value. NASA counter-part of peer-reviewed formal professional papers but has less stringent limitations on manuscript length and extent of graphic presentations.

- TECHNICAL MEMORANDUM. Scientific and technical findings that are preliminary or of specialized interest, e.g., quick release reports, working papers, and bibliographies that contain minimal annotation. Does not contain extensive analysis.

- CONTRACTOR REPORT. Scientific and technical findings by NASA-sponsored contractors and grantees.

- CONFERENCE PUBLICATION. Collected papers from scientific and technical conferences, symposia, seminars, or other meetings sponsored or co-sponsored by NASA.

- SPECIAL PUBLICATION. Scientific, technical, or historical information from NASA programs, projects, and missions, often concerned with subjects having substantial public interest.

- TECHNICAL TRANSLATION. English-language translations of foreign scientific and technical material pertinent to NASA's mission.

Specialized services also include organizing and publishing research results, distributing specialized research announcements and feeds, providing information desk and personal search support, and enabling data exchange services.

For more information about the NASA STI program, see the following:

- Access the NASA STI program home page at http://www.sti.nasa.gov

- E-mail your question to help@sti.nasa.gov

- Fax your question to the NASA STI Information Desk at 443-757-5803

- Phone the NASA STI Information Desk at 443-757-5802

- Write to:
  STI Information Desk
  NASA Center for AeroSpace Information
  7115 Standard Drive
  Hanover, MD 21076-1320

NASA/TM—2012–215972

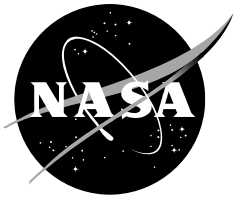

Design of Low Complexity Model Reference Adaptive Controllers

Curt Hanson and Jacob Schaefer
Dryden Flight Research Center, Edwards, California

Marcus Johnson and Nhan Nguyen
NASA Ames Research Center, Mountain View, California

National Aeronautics and
Space Administration

Dryden Flight Research Center
Edwards, CA 93523-0273

May 2012

Available from:

NASA Center for AeroSpace Information
7115 Standard Drive
Hanover, MD 21076-1320
443-757-5802

Abstract

Flight research experiments have demonstrated that adaptive flight controls can be an effective technology for improving aircraft safety in the event of failures or damage. However, the nonlinear, time-varying nature of adaptive algorithms continues to challenge traditional methods for the verification and validation testing of safety-critical flight control systems. Increasingly complex adaptive control theories and designs are emerging, but only make testing challenges more difficult. A potential first step toward the acceptance of adaptive flight controllers by aircraft manufacturers, operators, and certification authorities is a very simple design that operates as an augmentation to a non-adaptive baseline controller. Three such controllers were developed as part of a National Aeronautics and Space Administration flight research experiment to determine the appropriate level of complexity required to restore acceptable handling qualities to an aircraft that has suffered failures or damage. The controllers consist of the same basic design, but incorporate incrementally-increasing levels of complexity. Derivations of the controllers and their adaptive parameter update laws are presented along with details of the controllers' implementations.

Nomenclature

Acronyms

FAST	full-scale advanced systems testbed
IFCS	intelligent flight control system
IRAC	intelligent resilient aircraft control
MRAC	model reference adaptive control
NASA	National Aeronautics and Space Administration
NDI	nonlinear dynamic inversion
OCM	optimal control modification
onMRAC	MRAC with normalization and OCM
onMRAC+	MRAC with normalization, OCM and additional adaptive parameters
RFI	request for information
SDC	self designing controller
sMRAC	simple MRAC

Mathematical Symbols

A	matrix of state derivative coefficients
B	matrix of input coefficients
C	output error feedback compensator
f_A	applied aerodynamic and inertial moments
$\hat{f}_A$	estimate of applied aerodynamic and inertial moments
H	angular momentum vector
I	inertia matrix
k	reference model forward path gain
$\bar{k}$	uncertain forward path gain
L_α	reference model apparent lift curve slope
$\bar{L}_\alpha$	uncertain apparent lift curve slope
m	number of control effectors
M	vector of applied moments
N	control weighting matrix

p	roll rate
p_q	individual element of the matrix solution to the pitch axis Lyapunov equation
$\tilde{p}$	roll rate tracking error
$\dot{p}$	roll acceleration
$\dot{\tilde{p}}$	roll acceleration tracking error
P	solution to the Lyapunov equation
q	pitch rate
q_q	individual element of the pitch axis Lyapunov equation matrix
$\tilde{q}$	pitch rate tracking error
$\dot{q}$	pitch acceleration
$\dot{\tilde{q}}$	pitch acceleration error
Q	right-hand-side term of the Lyapunov equation
r	reference model input
r_{max}	maximum achievable yaw rate
$\bar{r}$	uncertain reference input
$\dot{r}$	yaw acceleration
R	reference model
s	Laplace operator
t	time
u	scalar control input
V	Lyapunov function
$\dot{V}$	Lyapunov function derivative
x	state vector
$\dot{x}$	state derivative vector
$\tilde{x}$	state error vector
$\dot{\tilde{x}}$	derivative of the state error vector
y	output vector
α	angle of attack
γ	adaptive parameter learning rate
Γ	matrix of adaptive parameter learning rates
δ	surface command vector
δ_{ap}	pilot roll stick input
δ_{ep}	pilot pitch stick input
Δ	moments due to external disturbances
ζ	reference model damping ratio
$\bar{\zeta}$	uncertain damping ratio
θ	matched uncertainty parameter
$\hat{\theta}$	matched uncertainty parameter adaptive estimate
$\tilde{\theta}$	matched adaptive parameter estimate error
Θ	vector of matched uncertainty parameters
$\dot{\Theta}$	vector of matched uncertainty parameter derivatives
$\hat{\dot{\Theta}}$	vector of matched uncertainty parameter derivative estimates
$\tilde{\Theta}$	vector of matched uncertainty parameter estimate errors
$\dot{\tilde{\Theta}}$	vector of matched uncertainty parameter estimate error derivatives
μ	forward path gain uncertainty
μ_L	apparent lift curve slope uncertainty
ν	optimal control modification tuning gain
σ	scalar time-varying uncertain disturbance

$\hat{\sigma}$	scalar time-varying uncertain disturbance adaptive estimate
$\dot{\hat{\sigma}}$	scalar time-varying uncertain disturbance adaptive estimate derivative
$\tilde{\sigma}$	scalar time-varying uncertain disturbance adaptive estimate error
$\dot{\tilde{\sigma}}$	scalar time-varying uncertain disturbance adaptive estimate error derivative
ω	reference model undamped natural frequency
$\overline{\omega}$	uncertain undamped natural frequency
Ω	vector of body-axis rotational rates
$\dot{\Omega}$	vector of body-axis rotational accelerations

Subscripts

0	trim
a	adaptive augmentation
c	compensator augmentation
cmd	command
err	NDI reference model tracking error
m	MRAC reference model
p	roll axis
q	pitch axis
ref	NDI reference model
δ	surface commands
θ	matched uncertainties
σ	uncertain disturbance

Superscript

n	number of reference model states

Introduction

Flight research of adaptive control algorithms has been sporadic over the past 50 years, providing relatively little flight data to guide present-day designers on their application to full-scale piloted aircraft. Examples that do exist include the first flight tests of a model reference adaptive controller on the F-94A aircraft (Lockheed Martin, Bethesda, Maryland) (ref 1), an experimental adaptive flight control system evaluated on the F-94C aircraft (Lockheed Martin, Bethesda, Maryland) (ref. 2), the implementation of an adaptive flight control system on the X-15 aircraft (North American Aviation Inc., Downy, California) (refs. 3, 4), testing of an indirect-adaptive self designing controller (SDC) on the F-16 VISTA (General Dynamics, now Lockheed Martin, Bethesda, Maryland) (ref. 5) and the intelligent flight control system (IFCS) research on the highly-modified National Aeronautics and Space Administration (NASA) F-15 aircraft (McDonnell Douglas, now The Boeing Company, Chicago, Illinois) (refs. 6, 7) . By the mid-2000s, experiments such as SDC and IFCS had demonstrated that adaptive flight controls can be an effective technology for improving aircraft safety in the event of failures or damage. However, the nonlinear, time-varying nature of adaptive systems continues to challenge traditional methods for the verification and validation of safety-critical flight control systems.

In April of 2009, NASA's Integrated Resilient Aircraft Control (IRAC) project disseminated a request for information (RFI) to the adaptive controls community seeking ideas for potential flight experiments (ref. 8). A workshop was held in Chicago in August of 2009 with representatives from industry, academia and other government agencies to discuss the wide variety of RFI responses received by NASA. Three focus areas were identified through this process.

1. Simple, yet effective, adaptive control algorithms should be investigated to help address the issue of verification and validation of adaptive flight controls to a safety-critical level.

2. The appropriate level of pilot awareness and interaction with adaptive control systems should be studied, including the potential for adverse interactions such as pilot-in-the-loop oscillations.

3. Techniques should be matured for incorporating feedback information, both static and dynamic, from an aircraft's structure into the flight control system.

The first, and to some extent, the second of these focus areas prompted the application of a low complexity, textbook-like direct model reference adaptive control (MRAC) scheme to the NASA Full-Scale Advanced Systems Testbed (FAST). FAST is a highly modified F-18 aircraft (McDonnell-Douglas, now The Boeing Company, Chicago, Illinois) that contains a research flight control system capable of housing advanced flight controls experiments. Full-scale piloted in-flight experimentation of adaptive systems has been shown to uncover implementation issues that may not be found through experiments with simulations or sub-scale, remotely piloted aircraft (refs 1, 4-7). Three variations of a low complexity MRAC design were evaluated for a healthy airplane and five simulated failure scenarios, characterized by a severe loss of damping in either the pitch or the roll axis, a loss of static pitch stability, a failed stabilator, and coupling from the roll axis into the pitch axis.

A philosophy of "simpler is better" motivated the development of the low complexity MRAC formulation under the assumption that simplification leads to lower implementation and verification costs, and ultimately to a greater likelihood of acceptance by aircraft manufacturers, operators and certification authorities. Reduced complexity can also lead to a safer design by reducing the potential for implementation errors within the adaptive controller software.

Evaluation of the relative complexity of various control techniques, including adaptive control methods, requires metrics for measuring complexity as it relates to design, implementation, software qualification, and flight testing. Various levels of reduced complexity were achieved for the three adaptive controllers through the incremental minimization of the following categories of elements common to most flight control systems.

1. Mathematical constructs such as integrators and filters require initialization or internal state limiting, and so their implementation requires special attention during design and testing. Other examples include inverse functions which must be protected from divide-by-zero scenarios.

2. Free design parameters such as gains, learning rates, and filter coefficients are elements of the controller that must be tuned to achieve the desired combination of controller performance and robustness. Increasing the number of free design parameters tends to complicate the design and verification effort of the controller due to the potential for unforeseen interactions and the increased difficulty of intuitively identifying cause and effect.

3. Input / output plane dimensionality of the adaptive controller impacts control system analysis and testing. Robustness analysis is typically performed at each feedback loop and each output. Noise, latency, and sampling rate characteristics must be evaluated and analyzed for each input and actuator dynamics included for each output. During development and testing, the failure mode of each input and output must be characterized, and their effects considered.

Three variations of a model reference adaptive control design were implemented as pilot-selectable augmentation modes to a non-adaptive baseline, nonlinear dynamic inversion (NDI) controller. This

approach is representative of a pilot-initiated emergency mode. Figure 1 shows the top-level block diagram of the integrated NDI and MRAC controllers. The simplest design consisted of a single adaptive parameter in each of the pitch and roll axes, computed using a basic gradient-based update law. A second design increased the complexity of the update law, while the third included one additional adaptive parameter in each axis.

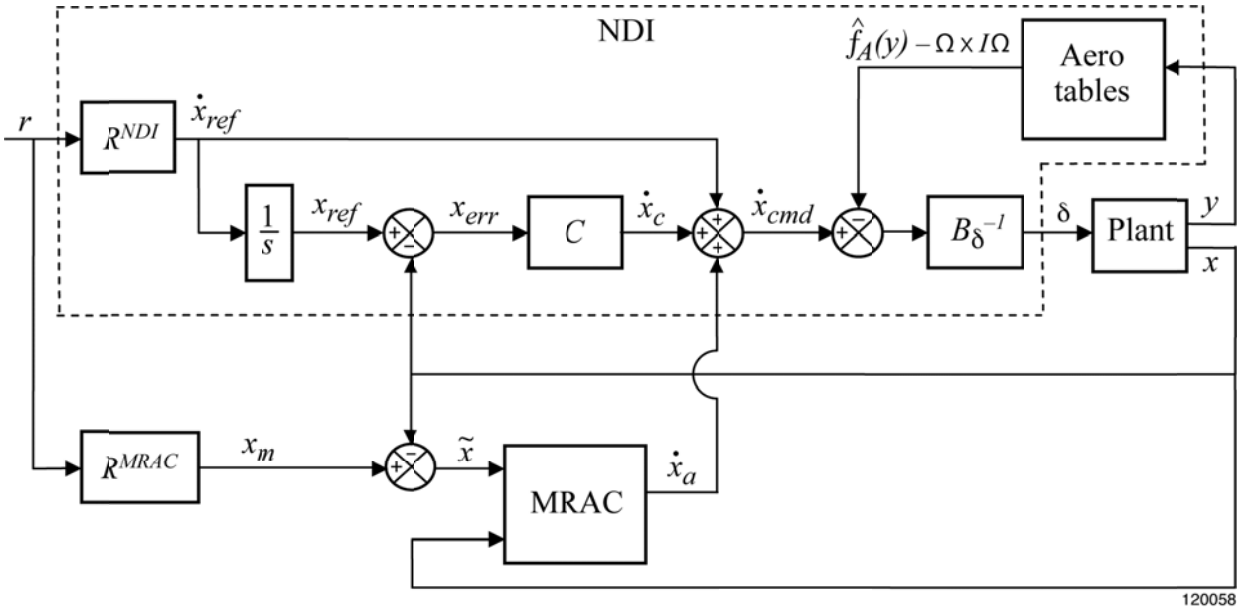

Figure 1. MRAC with NDI block diagram.

Nonlinear Dynamic Inversion Controller Description

The non-adaptive baseline is a full, nonlinear dynamic inversion inner-loop controller. The NDI inner-loop includes a proportional-plus-integral output error feedback compensator for improved robustness. NDI was chosen for its analyzability and open-source architecture. Furthermore, its explicit model-following architecture and on-board aerodynamic lookup tables provide convenient methods for introducing simulated aircraft failures and damage.

NDI inverts the aircraft equations of motion to compute appropriate control surface commands. The rotational equations of motion for an aircraft can be written using the relationship between the rate of change of momentum and applied moments under the assumption of constant inertias (ref. 9):

$$\frac{d}{dt}H(t) = I\dot{\Omega}(t) + \Omega(t) \times I\Omega(t) = \sum M(t) \tag{1}$$

Equation (1) is solved for the rotational acceleration vector $I\dot{\Omega}(t)$ as a function of the inertial coupling terms $\Omega(t) \times I\Omega(t)$ and the applied moments $\sum M(t)$. The applied moments term is expanded into the applied aerodynamic and inertial moments f_A, the applied moments due to control surface deflections $B_\delta(\delta(t) - \delta_0)$, and applied moments due to disturbances $\Delta(t)$.

$$I\dot{\Omega}(t) = f_A\big(y(t)\big) + B_\delta(\delta(t) - \delta_0) - \Omega(t) \times I\Omega(t) - \Delta(t) \tag{2}$$

Here, $y(t)$ is the output vector consisting of rotational body rates and the aerodynamic angles of attack and sideslip. The rotational acceleration vector $\dot{\Omega}(t)$ on the left-hand side is replaced by the vector of desired rotational acceleration commands $\dot{x}_{cmd}(t)$. The aerodynamic and inertial moments are replaced with an estimate $\hat{f}_A\big(y(t)\big)$ computed from on-board aerodynamic lookup tables. Equation (2) is then solved for the control surface deflection vector $\delta(t)$ necessary to achieve the commanded dynamics. When computing the commands, the disturbance term $\Delta(t)$ is assumed to be zero because it is generally not known.

$$\delta(t) = B_\delta^{-1}\left(I\dot{x}_{cmd}(t) + \Omega(t) \times I\Omega(t) - \hat{f}_A\big(y(t)\big)\right) + \delta_0 \tag{3}$$

Uncertainty in aerodynamic lookup tables or the presence of a non-zero disturbance $\Delta(t)$ will produce errors in the inverted dynamics of equation (3). A proportional-plus-integral output error feedback compensator C is added to reduce the inversion errors and improve model following. Similarly, adaptive feedback compensation can be added to account for larger errors due to failures or damage. Equation (4) gives the expanded acceleration command vector for each axis. Note that in equation (4) the $\dot{x}_{ref}(t)$ terms are the outputs of the reference model in figure 1, the $\dot{x}_c(t)$ terms are the outputs of the error compensator C, and the $\dot{x}_a(t)$ terms are the adaptive control contributions. Additional details on the NDI implementation can be found in Miller (ref. 10).

$$\dot{x}_{cmd}(t) = \dot{x}_{ref}(t) + \dot{x}_c(t) + \dot{x}_a(t) = \begin{bmatrix} \dot{p}_{ref}(t) + \dot{p}_c(t) + \dot{p}_a(t) \\ \dot{q}_{ref}(t) + \dot{q}_c(t) + \dot{q}_a(t) \\ \dot{r}_{ref}(t) + \dot{r}_c(t) \end{bmatrix} \tag{4}$$

The NDI controls all three axes, although adaptive augmentation is applied only to the pitch and roll axes of the aircraft, as the characteristics of these axes tend to dominate the pilot's perception of handling qualities for the proposed set of flight maneuvers. The relative benefits of incorporating yaw-axis adaptation were extensively debated by the design team. Ultimately, in keeping with the philosophy of simplification, yaw-axis adaptation was not included so that related performance deficiencies, if any, might be definitively revealed through flight test, at least for the proposed set of simulated failures and aircraft maneuvers.

General Description of the Low Complexity Model Reference Adaptive Controller

Model reference adaptive control (MRAC) derives its name from the use of reference model dynamics to define a desired trajectory for the system outputs to follow (ref. 11). The reference model for the aircraft axis of interest is specified as a stable, linear time-invariant system:

$$\dot{x}_m(t) = A_m x_m(t) + B_m r(t) \tag{5}$$

The scalar reference input $r(t)$ in equation (5) is a function of the time-varying pilot control command. Constant matrices $A_m \in \mathbb{R}^{n\times n}$ and $B_m \in \mathbb{R}^{n\times 1}$ are selected to give good aircraft handling qualities. The aircraft's true dynamics, which are uncertain and possibly unstable, may be written as

$$\dot{x}(t) = Ax(t) + B\big(u(t) - \sigma(t)\big) \tag{6}$$

where A and B are unknown and $\sigma(t)$ is a scalar, time-varying uncertain disturbance. The unknown aircraft dynamics and known reference model dynamics are related according to the MRAC matching conditions (ref. 11):

$$A = A_m - B\Theta^T \tag{7}$$

$$B = B_m \tag{8}$$

Several restrictions are apparent from the matching conditions in equations (7) and (8). The order n of the reference model must match the order of the aircraft dynamics described by equation (6), which also defines the number of matched uncertainties in the parameter vector Θ. These uncertainties, commonly referred to as A-matrix uncertainties, are additive and parameterize changes to the aircraft's pitch and roll dynamics. It is assumed that these uncertainties are either constant or that they vary slowly in comparison to the aircraft's dynamics. The *B*-matrices are assumed to be identical so that any differences in control effectiveness are parameterized as exogenous disturbances, as discussed below.

Parameterization of Pitch Axis Uncertainty

The typical representation of an aircraft's pitch-axis short-period dynamics is as a second-order transfer function (ref. 12). Let equation (9) represent the desired dynamics defined by the reference model, while the uncertain pitch dynamics (without external disturbances) are given by equation (10).

$$\frac{q_m(s)}{\delta_{ep}(s)} = \frac{k_q\omega_q^2(s + L_\alpha)}{s^2 + 2\zeta_q\omega_q s + \omega_q^2} \tag{9}$$

$$\frac{q(s)}{\delta_{ep}(s)} = \frac{\bar{k}_q\bar{\omega}_q^2(s + \bar{L}_\alpha)}{s^2 + 2\bar{\zeta}_q\bar{\omega}_q s + \bar{\omega}_q^2} \tag{10}$$

Equations (9) and (10) can be written in the state space form of equations (5) and (6), with the introduction of an unknown external disturbance Δ_q in the aircraft's true dynamics.

$$\begin{bmatrix} q_m(t) \\ \dot{q}_m(t) \end{bmatrix} = \begin{bmatrix} 0 & 1 \\ -\omega_q^2 & -2\zeta_q\omega_q \end{bmatrix} \begin{bmatrix} \int q_m(t) \\ q_m(t) \end{bmatrix} + \begin{bmatrix} 0 \\ 1 \end{bmatrix} k_q\omega_q^2 \left(\delta_{ep}(t) + L_\alpha \int \delta_{ep}(t) \right) \tag{11}$$

$$\begin{bmatrix} q(t) \\ \dot{q}(t) \end{bmatrix} = \begin{bmatrix} 0 & 1 \\ -\bar{\omega}_q^2 & -2\bar{\zeta}_q\bar{\omega}_q \end{bmatrix} \begin{bmatrix} \int q(t) \\ q(t) \end{bmatrix} + \begin{bmatrix} 0 \\ 1 \end{bmatrix} \left(\bar{k}_q\bar{\omega}_q^2 \left(\delta_{ep}(t) + \bar{L}_\alpha \int \delta_{ep}(t) \right) - \Delta_q \right) \tag{12}$$

The MRAC matching condition in equation (7) can now be used to parameterize the pitch axis matched uncertainty using the *A*-matrices from equations (11) and (12), where $B = B_q = [0 \quad 1]^T$ and $\Theta^T = \Theta_q^T = [\theta_{q1} \quad \theta_{q2}]$. Equation (13) shows that the uncertainty term θ_{q1} corresponds to uncertainty in the short period natural frequency and that θ_{q2} represents uncertainty in both the short period frequency and damping.

$$\begin{bmatrix} 0 & 1 \\ -\bar{\omega}_q^2 & -2\bar{\zeta}_q\bar{\omega}_q \end{bmatrix} = \begin{bmatrix} 0 & 1 \\ -\left(\omega_q^2 + \theta_{q1}\right) & -\left(2\zeta_q\omega_q + \theta_{q2}\right) \end{bmatrix} \tag{13}$$

Define the reference input signal for the reference model according to equation (14) and for the uncertain pitch dynamics by equation (15).

$$r_q(t) = k_q\omega_q^2\left(\delta_{ep}(t) + L_\alpha\int \delta_{ep}(t)\right) \tag{14}$$

$$\bar{r}_q(t) = \bar{k}_q\bar{\omega}_q^2\left(\delta_{ep}(t) + \bar{L}_\alpha\int \delta_{ep}(t)\right) \tag{15}$$

The total input uncertainty is parameterized by writing the entire input expression $\bar{r}_q(t) - \Delta_q(t)$ of equation (12) in terms of the known reference input $r_q(t)$ and the uncertainty parameter $\sigma_q(t)$:

$$\bar{r}_q(t) - \Delta_q(t) = r_q(t) - \sigma_q(t) \tag{16}$$

Insight into $\sigma_q(t)$ can be found by re-arranging equation (16) and writing it in terms of the known components of equation (14) and uncertainty parameters for feed-forward gain uncertainty μ_q, the apparent lift curve slope uncertainty μ_L and external disturbances $\Delta_q(t)$.

$$\sigma_q(t) = k_q\omega_q^2[1 \quad -\mu_q]\begin{bmatrix}1 & L_\alpha \\ 1 & L_\alpha - \mu_L\end{bmatrix}\begin{bmatrix}\delta_{ep}(t) \\ \int \delta_{ep}(t)\end{bmatrix} + \Delta_q(t) \tag{17}$$

The feed-forward gain and apparent lift curve slope uncertainty parameters are defined in equations (18) and (19), respectively. It will be shown that the adaptive controller does not estimate each of these uncertainties independently, but rather computes the aggregate estimate $\hat{\sigma}_q(t)$.

$$\mu_q = \frac{\bar{k}_q\bar{\omega}_q^2}{k_q\omega_q^2} \tag{18}$$

$$\mu_L = (L_\alpha - \bar{L}_\alpha) \tag{19}$$

Parameterization of Roll Axis Uncertainty

A first-order transfer function is used to model the stability axis roll dynamics (ref. 10). Let equation (20) represent the known desired dynamics and equation (21) represent the unknown roll axis dynamics (again without external disturbances).

$$\frac{p_m(s)}{\delta_{ap}(s)} = \frac{\left(\frac{r_{max}}{\alpha}\right)k_p\omega_p}{s + \omega_p} \tag{20}$$

$$\frac{p(s)}{\delta_{ap}(s)} = \frac{\left(\frac{r_{max}}{\alpha}\right)\bar{k}_p\bar{\omega}_p}{s + \bar{\omega}_p} \tag{21}$$

Following the approach used in the pitch axis, equations (20) and (21) are written in state space notation, with the introduction of the external disturbance term $\Delta_p(t)$.

$$\dot{p}_m(t) = \left[-\omega_p\right]p_m(t) + [1]\left(\frac{r_{max}}{\alpha(t)}\right)k_p\omega_p\delta_{ap}(t) \tag{22}$$

$$\dot{p}(t) = \left[-\bar{\omega}_p\right]p(t) + [1]\left(\left(\frac{r_{max}}{\alpha(t)}\right)\bar{k}_p\bar{\omega}_p\delta_{ap}(t) - \Delta_p(t)\right) \tag{23}$$

The MRAC matching condition of equation (7) is used to parameterize the roll axis uncertainty, where $B = B_p = [1]$ and $\Theta = \Theta_p = \theta_p$.

$$-\bar{\omega}_p = -\left(\omega_p + \theta_p\right) \tag{24}$$

Define the reference input signal for the reference model according to equation (25) and for the uncertain roll dynamics according to equation (26).

$$r_p(t) = \left(\frac{r_{max}}{\alpha(t)}\right) k_p \omega_p \delta_{ap}(t) \tag{25}$$

$$\bar{r}_p(t) = \left(\frac{r_{max}}{\alpha(t)}\right) \bar{k}_p \bar{\omega}_p \delta_{ap}(t) \tag{26}$$

The total input uncertainty is parameterized by writing the entire input expression $\bar{r}_p(t) - \Delta_p(t)$ of equation (23) in terms of the known reference input $r_p(t)$ and the uncertainty parameter $\sigma_p(t)$:

$$\bar{r}_p(t) - \Delta_p(t) = r_p(t) - \sigma_p(t) \tag{27}$$

The uncertainty term σ_p contains the term μ_p, which is a parameterization of uncertainty in the gain between the known and unknown reference input signals of equations (25) and (26), as well as the external roll disturbance $\Delta_p(t)$.

$$\sigma_p(t) = \left(\frac{r_{max}}{\alpha(t)}\right) k_p \omega_p \left(1 - \mu_p\right) \delta_{ap}(t) + \Delta_p(t) \tag{28}$$

The roll feed forward gain uncertainty is defined as

$$\mu_p = \frac{\bar{k}_p \bar{\omega}_p}{k_p \omega_p} \tag{29}$$

Adaptive Control Commands

The scalar control input $u(t)$ in equation (6) for the pitch axis is defined to be a combination of the scalar reference input and augmentation from the adaptive controller.

$$u_q(t) = r_q(t) + \dot{q}_a(t) = r_q(t) + \begin{bmatrix} \hat{\theta}_{q1}(t) & \hat{\theta}_{q2}(t) \end{bmatrix} \begin{bmatrix} \int q(t) \\ q(t) \end{bmatrix} + \hat{\sigma}_q(t) \tag{30}$$

Adaptive parameters $\hat{\theta}_{q1}(t)$, $\hat{\theta}_{q2}(t)$ and $\hat{\sigma}_q(t)$ are estimates of the θ_{q1}, θ_{q2} and σ_q uncertainties. The control input from equation (30) is substituted into the pitch axis form of equation (6) along with the matching condition of equation (13) to find

$$\begin{bmatrix} q(t) \\ \dot{q}(t) \end{bmatrix} = \begin{bmatrix} 0 & 1 \\ -\left(\omega_q^2 + \theta_{q1}\right) & -\left(2\zeta_q \omega_q + \theta_{q2}\right) \end{bmatrix} \begin{bmatrix} \int q(t) \\ q(t) \end{bmatrix} + \begin{bmatrix} 0 \\ 1 \end{bmatrix} \left(r_q(t) + \begin{bmatrix} \hat{\theta}_{q1}(t) & \hat{\theta}_{q2}(t) \end{bmatrix} \begin{bmatrix} \int q(t) \\ q(t) \end{bmatrix} + \hat{\sigma}_q(t) - \sigma_q(t) \right) \tag{31}$$

Re-arrange to combine similar terms.

$$\begin{bmatrix} q(t) \\ \dot{q}(t) \end{bmatrix} = \begin{bmatrix} 0 & 1 \\ -\omega_q^2 - \left(\theta_{q1} - \hat{\theta}_{q1}(t)\right) & -2\zeta_q\omega_q - \left(\theta_{q2} - \hat{\theta}_{q2}(t)\right) \end{bmatrix} \begin{bmatrix} \int q(t) \\ q(t) \end{bmatrix} + \begin{bmatrix} 0 \\ 1 \end{bmatrix} \left(r_q(t) - \left(\sigma_q(t) - \hat{\sigma}_q(t) \right) \right) \tag{32}$$

The control objective is that as adaptation takes place, $\hat{\theta}_{q1}(t) \to \theta_{q1}$, $\hat{\theta}_{q2}(t) \to \theta_{q2}$ and $\hat{\sigma}(t) \to \sigma(t)$ so that the dynamics of equation (33) approach the desired reference dynamics of equation (11).

$$\begin{bmatrix} q(t) \\ \dot{q}(t) \end{bmatrix} = \begin{bmatrix} 0 & 1 \\ -\omega_q^2 & -2\zeta_q\omega_q \end{bmatrix} \begin{bmatrix} \int q(t) \\ q(t) \end{bmatrix} + \begin{bmatrix} 0 \\ 1 \end{bmatrix} r_q(t) \tag{33}$$

The roll axis scalar control input $u_p(t)$ contains the reference input and two adaptive parameters.

$$u_p(t) = r_p(t) + \dot{p}_a(t) = r_p(t) + \hat{\theta}_p(t)p(t) + \hat{\sigma}_p(t) \tag{34}$$

Under the control signal of equation (34) the roll axis dynamics can be written as

$$\dot{p}(t) = \left[-\omega_p - \left(\theta_p - \hat{\theta}_p(t) \right) \right] p(t) + [1] \left(r_p(t) - \left(\sigma_p(t) - \hat{\sigma}_p(t) \right) \right) \tag{35}$$

Similar to the pitch axis, as $\hat{\theta}_p \to \theta_p$ and $\hat{\sigma}_p \to \sigma_p$ the airplane roll axis dynamics match the desired reference model dynamics in equation (22).

$$\dot{p}(t) = \left[-\omega_p \right] p(t) + [1] r_p(t) \tag{36}$$

Basic Adaptive Parameter Update Laws

The three adaptive control designs all employ variations of the same basic adaptive parameter update laws, developed in this section.

Pitch Axis MRAC

Pitch axis tracking error is computed by subtracting the aircraft response from the desired dynamics of the reference model.

$$\tilde{x}_q(t) = \begin{bmatrix} \int \tilde{q}(t) \\ \tilde{q}(t) \end{bmatrix} = \begin{bmatrix} \int q_m(t) \\ q_m(t) \end{bmatrix} - \begin{bmatrix} \int q(t) \\ q(t) \end{bmatrix} \tag{37}$$

Differentiate equation (37) and substitute equations (11), (14) and (32), making the following definitions: $\tilde{\theta}_{q1}(t) = \theta_{q1} - \hat{\theta}_{q1}(t)$, $\tilde{\theta}_{q2}(t) = \theta_{q2} - \hat{\theta}_{q2}(t)$ and $\tilde{\sigma}_q(t) = \sigma_q(t) - \hat{\sigma}_q(t)$.

$$\begin{bmatrix}\tilde{q}(t)\\ \dot{\tilde{q}}(t)\end{bmatrix} = \begin{bmatrix}0 & 1\\ -\omega_q^2 & -2\zeta_q\omega_q\end{bmatrix}\begin{bmatrix}\int q_m(t)\\ q_m(t)\end{bmatrix} + \begin{bmatrix}0\\1\end{bmatrix} r_q(t) - \begin{bmatrix}0 & 1\\ -\omega_q^2 - \tilde{\theta}_{q1}(t) & -2\zeta_q\omega_q - \tilde{\theta}_{q2}(t)\end{bmatrix}\begin{bmatrix}\int q(t)\\ q(t)\end{bmatrix} - \begin{bmatrix}0\\1\end{bmatrix}\left(r_q(t) - \tilde{\sigma}_q(t)\right) \tag{38}$$

Equation (38) can be re-arranged to form the following expression for the pitch axis error dynamics.

$$\dot{\tilde{x}}_q(t) = A_{m_q}\tilde{x}_q(t) + B_{m_q}\widetilde{\Theta}_q^T(t)x_q(t) + B_{m_q}\tilde{\sigma}_q(t) \tag{39}$$

Define the following Lyapunov function according to equation (40), where $P_q = P_q^T \in \mathbb{R}^{2\times2}$ and is positive definite. Note also that the positive definite matrix $\Gamma_{\theta_q} \in \mathbb{R}^{2\times2}$ and that $\gamma_{\sigma_q} \in \mathbb{R}^+$. The matrices Γ_{θ_q} and P_q are defined in equations (41) and (42) respectively.

$$V_q(t) = \tilde{x}_q^T(t)P_q\tilde{x}_q(t) + \widetilde{\Theta}_q^T(t)\Gamma_{\theta_q}^{-1}\widetilde{\Theta}_q(t) + \frac{\tilde{\sigma}_q^2(t)}{\gamma_{\sigma_q}} \tag{40}$$

$$\Gamma_{\theta_q} = \begin{bmatrix}\gamma_{\theta_{q1}} & 0\\ 0 & \gamma_{\theta_{q2}}\end{bmatrix} \tag{41}$$

$$P_q = \begin{bmatrix}p_q^{11} & p_q^{12}\\ p_q^{12} & p_q^{22}\end{bmatrix} \tag{42}$$

Differentiate equation (40).

$$\dot{V}_q(t) = \dot{\tilde{x}}_q^T(t)P_q\tilde{x}_q(t) + \tilde{x}_q^T(t)P_q\dot{\tilde{x}}_q(t) + 2\widetilde{\Theta}_q^T(t)\Gamma_{\theta_q}^{-1}\dot{\widetilde{\Theta}}_q(t) + \frac{2\tilde{\sigma}_q(t)\dot{\tilde{\sigma}}_q(t)}{\gamma_{\sigma_q}} \tag{43}$$

Substitute $\dot{\tilde{x}}_q(t)$ and $\dot{\tilde{x}}_q^T(t)$ from equation (39) to get equation (44).

$$\begin{aligned}\dot{V}_q(t) = {} & \tilde{x}_q^T(t)A_{m_q}^TP_q\tilde{x}_q(t) + x_q^T(t)\widetilde{\Theta}_q(t)B_{m_q}^TP_q\tilde{x}_q(t) + \tilde{\sigma}_q(t)B_{m_q}^TP_q\tilde{x}_q(t)\\ & + \tilde{x}_q^T(t)P_qA_{m_q}\tilde{x}_q(t) + \tilde{x}_q^T(t)P_qB_{m_q}\widetilde{\Theta}_q^T(t)x_q(t) + \tilde{x}_q^T(t)P_qB_{m_q}\tilde{\sigma}_q(t)\\ & + 2\widetilde{\Theta}_q^T(t)\Gamma_{\theta_q}^{-1}\dot{\widetilde{\Theta}}_q(t) + \frac{2\tilde{\sigma}_q(t)\dot{\tilde{\sigma}}_q(t)}{\gamma_{\sigma_q}}\end{aligned} \tag{44}$$

Rearrange equation (44) to combine like terms, recognizing that $\tilde{x}_q^T(t)P_qB_{m_q}$ is a scalar and may be moved appropriately within the expression.

$$\begin{aligned}\dot{V}_q(t) = {} & \tilde{x}_q^T(t)\left(A_{m_q}^TP_q + P_qA_{m_q}\right)\tilde{x}_q(t) + 2\widetilde{\Theta}_q^T(t)\tilde{x}_q^T(t)P_qB_{m_q}x_q(t)\\ & + 2\tilde{\sigma}_q(t)\tilde{x}_q^T(t)P_qB_{m_q} + 2\widetilde{\Theta}_q^T(t)\Gamma_{\theta_q}^{-1}\dot{\widetilde{\Theta}}_q(t) + \frac{2\tilde{\sigma}_q(t)\dot{\tilde{\sigma}}_q(t)}{\gamma_{\sigma_q}}\end{aligned} \tag{45}$$

The Lyapunov stability criteria of $\dot{V}_q(t) \leq 0$ is partially satisfied by equation (45) if the matrix P_q is computed according to the Lyapunov equation $A_{m_q}^TP_q + P_qA_{m_q} = -Q_q$, where $Q_q$is positive definite

matrix of tunable design parameters. The Lyapunov stability proof is completed by defining the following adaptive parameter update laws for substitution into equation (45).

$$\dot{\tilde{\Theta}}_q(\mathrm{t}) = \left(\dot{\Theta}_q - \dot{\hat{\Theta}}_q(\mathrm{t})\right) \cong -\dot{\hat{\Theta}}_q(\mathrm{t}) = -\begin{bmatrix} \gamma_{\theta_{q1}} & 0 \\ 0 & \gamma_{\theta_{q2}} \end{bmatrix} \tilde{x}_q^T(t) P_q B_{m_q} x_q(t) \tag{46}$$

$$\dot{\tilde{\sigma}}_q(t) = \left(\dot{\sigma}_q - \dot{\hat{\sigma}}_q(t)\right) \cong -\dot{\hat{\sigma}}_q(t) = -\gamma_{\sigma_q} \tilde{x}_q^T(t) P_q B_{m_q} \tag{47}$$

It should be noted that the assumption that the adaptive parameter rates of change are equal to the corresponding parameterization errors derivatives in equations (46) and (47) does not hold if the uncertainties are not constant or slowly changing as compared to the convergence rate of the adaptive parameter estimates.

Roll Axis MRAC

Roll axis tracking error is computed by subtracting the aircraft response from the desired dynamics of the reference model.

$$\tilde{x}_p(t) = \tilde{p}(t) = p_m(t) - p(t) \tag{48}$$

Differentiate equation (48) and substitute equations (22), (25) and (35).

$$\dot{\tilde{p}}(t) = \left[-\omega_p\right] p_m(t) + [1] r_p(t) - \left(-\omega_p - \tilde{\theta}_p(t)\right) p(t) - [1]\left(r_p(t) - \tilde{\sigma}_p(t)\right) \tag{49}$$

Rearrange equation (49) into the following expression for the roll error dynamics.

$$\dot{\tilde{p}}(t) = A_{m_p} \tilde{p}(t) + B_{m_p} \tilde{\theta}_p(t) p(t) + B_{m_p} \tilde{\sigma}_p(t) \tag{50}$$

Define the following Lyapunov function where P_p, γ_{θ_p} and γ_{σ_p} are positive non-zero scalars.

$$V_p(t) = \tilde{p}^2(t) P_p + \frac{\tilde{\theta}_p^2(t)}{\gamma_{\theta_p}} + \frac{\tilde{\sigma}_p^2(t)}{\gamma_{\sigma_p}} \tag{51}$$

Differentiate equation (51).

$$\dot{V}_p(t) = 2\tilde{p}(t) P_p \dot{\tilde{p}}(t) + \frac{2\tilde{\theta}_P(t)\dot{\tilde{\theta}}_P(t)}{\gamma_{\theta_p}} + \frac{2\tilde{\sigma}_P(t)\dot{\tilde{\sigma}}_P(t)}{\gamma_{\sigma_p}} \tag{52}$$

Substitute equation (50) into equation (52).

$$\dot{V}_p(t) = 2\tilde{p}^2(t) P_p A_{m_p} + 2\tilde{p}(t) P_p B_{m_p} \tilde{\theta}_p(t) p(t) + 2\tilde{p}(t) P_p B_{m_p} \tilde{\sigma}_p(t) + \frac{2\tilde{\theta}_P(t)\dot{\tilde{\theta}}_P(t)}{\gamma_{\theta_p}} + \frac{2\tilde{\sigma}_P(t)\dot{\tilde{\sigma}}_P(t)}{\gamma_{\sigma_p}} \tag{53}$$

Apply the scalar Lyapunov relationship for the roll axis, $2P_pA_{m_p} = -Q_p$ where Q_p is a positive, non-zero scalar. Define the following adaptive parameter update laws for the roll axis.

$$\dot{\hat{\theta}}_p(t) = \left(\dot{\theta}_p - \dot{\hat{\theta}}_p(t)\right) \cong -\dot{\hat{\theta}}_p(t) = -\gamma_{\theta_p}\tilde{p}(t)P_pB_{m_p}p(t) \tag{54}$$

$$\dot{\hat{\sigma}}_p(t) = \left(\dot{\sigma}_p - \dot{\hat{\sigma}}_p(t)\right) \cong -\dot{\hat{\sigma}}_p(t) = -\gamma_{\sigma_p}\tilde{p}(t)P_pB_{m_p} \tag{55}$$

The assumption regarding constant or slowly-changing uncertainties described in the pitch axis discussion also applies in the roll axis.

MRAC Controller Implementation Details

Before describing each of the different adaptive controllers, it is important to discuss several implementation details that are common across all three designs. These features address performance and robustness problems discovered in the piloted simulation during the process of selecting the tunable parameters p and γ in equations (46), (47), (54) and (55). In essence they represent the necessary bridge between MRAC theory and practical application.

Addressing Bias in the Pitch Axis

During the initial implementation process, the presence of quasi-steady, non-zero signals during extended pitch maneuvers such as wind-up turns tended to prevent the adaptive parameters from converging to their ideal values. Improved adaptation was achieved by minimizing the influence of certain biased signals or by removing the biases directly.

During constant pitch rate maneuvers, the input $\int q(t)$ grows unboundedly and can quickly begin to dominate pitch axis adaptation, producing poor adaptation characteristics. One common implementation feature between all three MRAC designs is that the influences of the input $\int q(t)$ and its associated adaptive parameter $\hat{\theta}_{q1}(t)$ are trivialized. The marginalization of these components, accomplished via the Γ_{θ_q} and P_q matrices, effectively reduces the number of adaptive parameters in the pitch axis to one and similarly streamlines the input plane to consist of pitch rate feedback only.

The learning rate $\gamma_{\theta_{q1}}$ for the $\hat{\theta}_{q1}(t)$ adaptive parameter is set much smaller, at least three orders of magnitude, than the learning rate $\gamma_{\theta_{q2}}$ for the $\hat{\theta}_{q2}(t)$ parameter. Similarly, the gain p_q^{12} for the $\int q(t)$ input is designed to be much smaller, by at least two orders of magnitude, than the gain p_q^{22} for the $q(t)$ input. These parameters were not set identically to zero to avoid violating the requirement of positive definiteness on Γ_{θ_q} and P_q.

Removing the influence of $\hat{\theta}_{q1}(t)$ and $\int q(t)$ improved the controllers' adaptation characteristics in constant pitch rate maneuvers. However, there still remained a tendency for $\hat{\theta}_{q2}(t)$ to over-adapt during periods of quasi-steady, non-zero pitch rate. The reason for this becomes apparent by multiplying out the terms in equation (46) for $\dot{\hat{\theta}}_{q2}(t)$ under the assumption that $p_q^{12} \approx 0$ to yield the expression in equation (56).

$$\dot{\hat{\theta}}_{q2}(t) = \gamma_{\theta_{q2}}p_q^{22}\tilde{q}(t)q(t) \tag{56}$$

It was observed, for example, that in a windup turn the achieved pitch rate was generally somewhat less than the reference model command, causing both $\tilde{q}(t)$ and $q(t)$ to be consistently greater than zero. By definition, $\gamma_{\theta_{q2}}$ and p_q^{22} are also positive non-zero, resulting in steady positive growth of the adaptive parameter $\hat{\theta}_{q2}(t)$. An examination of the aircraft dynamics in equation (32) reveals that positive increases in $\hat{\theta}_{q2}(t)$ correlate to reductions in closed-loop damping. This is consistent with the behavior observed in the piloted simulation, where the aircraft would lose damping during windup turns, eventually becoming unstable in pitch. It should be noted that this phenomenon was generally only observed in the two controller designs that did not include an estimation of the $\hat{\sigma}_q(t)$ term. From equation (17) it can be seen that $\hat{\sigma}_q(t)$ compensates for uncertainty in the loop gain, which would drive the error $\tilde{q}$ to zero and avoid over-adaptation.

To address over adaptation of the $\hat{\theta}_{q2}(t)$ during constant pitch rate maneuvers, a high-pass filter was applied to the terms $\tilde{q}(t)$ and $q(t)$ in equation (56). The same high-pass filter was applied to the pitch rate feedback term $q(t)$ in the adaptive augmentation command of equation (30).

Addressing Bias in the Roll Axis

During extended steady-heading sideslip maneuvers in the piloted simulation, frequent over-adaptation of the roll axis adaptive parameter $\hat{\theta}_p(t)$ occurred, resulting in uncommanded roll excursions. The root cause was very similar to the bias issue with $\hat{\theta}_{q2}(t)$ described above, although the roll-axis issue was discovered first. Essentially, the steady non-zero roll stick input required to accomplish the sideslip maneuver produced a non-zero reference model command. However, in this maneuver the rudder pedals are used to prevent the airplane from rolling and to achieve the desired sideslip. This discrepancy between roll command and feedback produced a large non-zero roll error, which tended to drive the value of $\hat{\theta}_p(t)$ to extreme values if the roll rate was not kept precisely zero and ultimately a large roll acceleration command resulted.

Following the discovery of this anomaly, a high-pass filter for the roll axis was discussed, but eliminated from consideration due to uncertainty over how it might impact other aspects of roll-axis performance. In keeping with the philosophy of a minimum complexity controller, the seemingly simpler approach was selected of fading the roll axis tracking error to zero as a function of rudder pedal displacement. A gain on the error was linearly reduced from one to zero over the first 50 percent of the available rudder pedal displacement, and held at zero for displacements larger than 50 percent. This solution effectively prevented further uncommanded roll excursions during steady-heading sideslips.

Later in the tuning process when high-pass filters were being added to the pitch axis to address a similar problem, high-pass filters were again considered for the roll axis. However, because the existing rudder-pedal attenuation gain corrected the problems with steady-heading sideslips and no other issues were found in the roll axis during parameter tuning, high-pass filtering was not implemented in the roll axis. Ultimately, several events during flight research later pointed to high-pass filtering as a likely better solution than the one implemented.

1. It was observed during 2g air-to-air tracking that some of the test pilots used rudder pedals more extensively than anticipated, causing the rudder pedal attenuation gain to adversely impact roll-axis adaptation during these maneuvers.

2. During simulation training of a NASA guest (non-program) pilot, uncommanded rolls occurred repeatedly during windup turns with a simulated failed stabilator. The cause was

attributed to the unusually smooth and low-gain technique of this particular pilot, producing a bias scenario similar to the one described previously for $\hat{\theta}_{q2}(t)$.

3. A roll-axis pilot-in-the-loop oscillation occurred during a formation tracking maneuver in which the wingtip vortex of the lead airplane produced a roll bias on the test aircraft (ref. 13).

Error Signal Time Correlation

In the initial implementation, system transport delays and structural filter phase losses on measured feedback parameters produced systemic tracking error in both axes. The calculations for tracking error are given by equations (37) and (48) for pitch and roll respectively. Even under ideal aircraft responses that matched the desired reference model dynamics, tracking error persisted due to phase differences between the command and feedback. This persistent error tended to overdrive the adaptive gains, lower performance, and reduce robustness to time delays.

Multi-frame first-order holds were placed on $q_m(t)$ and $p_m(t)$ to better align those signals with their corresponding feedback signals. Each signal was delayed by 50 milliseconds, an amount that was determined empirically in the piloted simulation during the adaptive parameter tuning process.

Miscellaneous Features

Additional features that were integrated into the control system are as follows. Integration limits were applied to the adaptive parameters to prevent excessive control commands in the event of over-adaptation. Limits were set slightly higher than the largest parameter values that were observed during piloted simulation evaluation of simulated failure/damage scenarios.

Some control over the adaptive augmentation was given to the pilot, including the ability to turn the adaptive controller on and off, and to freeze the adaptive parameters through the use of a button on the control stick. These features fulfilled two purposes. First, the results of flight experimentation were enhanced by the ability to conduct back-to-back comparisons of a given configuration with and without adaptation. Freezing the weights allowed the pilot to conduct identification maneuvers, such as frequency sweeps with the control stick, without altering the state of the adaptive controller. The second advantage of these features was to study pilot interaction with the adaptive control system. Some questions of interest include evaluation of pilot-initiated adaptive control versus automatic initiation of adaptation, and whether it is advisable to freeze the adaptive controller once adequate tracking has been restored.

MRAC Designs of Varying Complexity

Three MRAC controllers were implemented and tested to explore the relationships between adaptive controller complexity and performance, robustness, and handling qualities. The three controllers were built upon each other by adding levels of complexity rather than implementing three entirely independent designs. In this way, the positive and negative effects of the additional complexity can be studied.

Free design parameters were tuned in a piloted simulation for acceptable response when no failures were present as well as across a wide variety of simulated failures and damage scenarios. Although there were many parameters common to all three controllers, these were tuned differently for each controller as the additional complexity components tended to significantly affect performance, and the parameter values were adjusted accordingly. Aggressive pilot inputs were used during tuning to stress the system, and parameters were adjusted to achieve the fastest adaptation possible without introducing undesirable side effects such as over-adaptation and actuator rate limiting. Additional metrics used during the tuning

process included the integral of the tracking error, empirically-determined gain and time delay margins, and pilot comments.

The adaptive parameter update laws given in equations (46), (47), (54) and (55) represent the basic starting point in the implementation of the three adaptive controllers for the experiment. Differences between the three adaptive controllers are described in the following sections.

Simple MRAC (sMRAC)

Two of the three controllers have essentially a single adaptive parameter in each axis, where $\hat{\theta}_{q1}(t)$ is trivialized in the pitch axis as described earlier, and γ_{σ_q} and γ_{σ_p} are set to zero to eliminate the adaptive parameters $\hat{\sigma}_q(t)$ and $\hat{\sigma}_p(t)$. The first of these designs, sMRAC, makes use of the simple adaptive parameter update laws as they are described in equations (46) and (54).

As an example, the pitch axis adaptive update law in equation (46) simplifies to equation (57) under the assumption that the off-diagonal terms of the tunable design matrix Q_q are zero. See Appendix A, Calculation of the P_q Matrix for solutions to the Lyapunov equation. For all three controllers, Q_q was chosen to be diagonal, although there is no requirement for it to be so. The gains q_q^{11} and q_q^{22} are the upper-left and lower right elements, respectively, of Q_q. These gains were set as $q_q^{11} = 0.01$ and $q_q^{22} = 1$ for all three controllers so that the influence of $\tilde{q}(t)$ is approximately three orders of magnitude greater than that of $\int \tilde{q}(t)$. The learning rate for sMRAC was selected as $\gamma_{\theta_{q2}} = 1$.

$$\dot{\hat{\theta}}_{q2}(t) = \tfrac{1}{2}\gamma_{\theta_{q2}}\left(q_q^{11}\left(\frac{1}{\omega_q^2}\right)\int \tilde{q}(t) + \left(q_q^{11}\left(\frac{1}{\omega_q^2}\right)\left(\frac{1}{2\zeta_q\omega_q}\right) + q_q^{22}\left(\frac{1}{2\zeta_q\omega_q}\right)\right)\tilde{q}(t)\right) q(t) \tag{57}$$

MRAC with Optimal Control Modification and Normalization (onMRAC)

The onMRAC controller incorporates an optimal control modification term (ref. 14) and normalization into the update laws, described by equations (58) and (59).

$$\begin{bmatrix}\dot{\hat{\theta}}_{q1}(t)\\ \dot{\hat{\theta}}_{q2}(t)\end{bmatrix} = \frac{\Gamma_{\theta_q}}{1 + x_q^T(t)N_{\theta_q}x_q(t)}\left(\tilde{x}_q^T(t)P_qB_{m_q}x_q(t) - \begin{bmatrix}\nu_{\theta_{q1}} & 0\\ 0 & \nu_{\theta_{q2}}\end{bmatrix} x_q(t)x_q^T(t)\begin{bmatrix}\hat{\theta}_{q1}(t)\\ \hat{\theta}_{q2}(t)\end{bmatrix} B_{m_q}^TP_qA_{m_q}^{-1}B_{m_q}\right) \tag{58}$$

$$\dot{\hat{\theta}}_p(t) = \frac{\gamma_{\theta_p}}{1 + p^2(t)N_{\theta_p}}\left(\tilde{p}(t)P_pB_{m_p}p(t) - \nu_{\theta_p}p^2(t)\hat{\theta}_p(t)B_{m_p}^TP_pA_{m_p}^{-1}B_{m_p}\right) \tag{59}$$

Optimal control modification (OCM) is an update law modification term that helps to alleviate over-adaptation and dampen oscillations in the adaptive parameters. In equations (58) and (59), the first term

within the parentheses is the standard update law and the second term is the optimal control modification. Taking the pitch axis as an example, an examination of the elements of the OCM term reveals that $B_{m_q}^T P_q A_{m_q}^{-1} B_{m_q}$ is a scalar with a value of $-\frac{1}{2} q_q^{11}$, where q_q^{11} is the upper-left element of the positive-definite diagonal matrix Q_q. The tunable OCM gain $\nu_{\theta_{q1}}$ was set to zero since the adaptive parameter $\hat{\theta}_{q1}$ was essentially zeroed out. The OCM expression for the $\hat{\theta}_{q2}(t)$ update law becomes $+\frac{1}{2} q_q^{11} \nu_{\theta_{q2}} \hat{\theta}_{q2}(t) q^2(t)$ under the assumption that $\hat{\theta}_{q1}(t) \cong 0$. In the final design, $q_q^{11} = 0.01$ and $\nu_{\theta_{q2}} = -200$ so that the OCM term was simply $-\hat{\theta}_{q2}(t) q^2(t)$.

Normalization suppresses adaptation during large dynamic maneuvers through attenuation of the learning rate by the inverse of the weighted square of the feedback parameters. Squaring the input vector ensures that it is always positive, and weighting allows the designer to control the relative influence of each feedback term on the normalizing behavior. In the pitch axis onMRAC update law, the relative influence of the $\int q(t)$ term was kept very low. The normalization terms are also biased by a constant of one to prevent a divide-by-zero when the feedback vectors are zero. Inclusion of OCM and normalization allowed the learning rate $\gamma_{\theta_{q2}}$ to be increased from 1 to 50, enabling faster adaptation.

MRAC plus Adaptation for Disturbances (onMRAC+)

The third and most complex of the three controllers maintained the same update laws and tuning parameters as onMRAC for $\hat{\theta}_{q1}(t)$, $\hat{\theta}_{q2}(t)$ and $\hat{\theta}_p(t)$ while adding update laws for $\hat{\sigma}_q(t)$ and $\hat{\sigma}_p(t)$, given by equations (60) and (61).

$$\dot{\hat{\sigma}}_q(t) = \frac{\gamma_{\sigma_q}}{1 + x_q^T(t) N_{\sigma_q} x_q^T(t)} \tilde{x}_q^T(t) P_q B_{m_q} \tag{60}$$

$$\dot{\hat{\sigma}}_p(t) = \frac{\gamma_{\sigma_p}}{1 + p^2(t) N_{\sigma_p}} \left(\tilde{p}(t) P_p B_{m_p} + \nu_{\sigma_p} \hat{\sigma}_p B_{m_p}^T P_p A_{m_p}^{-1} B_{m_p} \right) \tag{61}$$

Normalization was found during the design process to improve the adaptation characteristics of both $\hat{\sigma}_q(t)$ and $\hat{\sigma}_p(t)$. Without normalization, high-rate pilot inputs produced excessively large transient values of both terms. Tuning of the learning rates γ_{σ_q} and γ_{σ_p} was insufficient to eliminate these transients without simultaneously making the adaptive parameters ineffective. Normalization allowed sufficiently fast adaptation without excessive transients.

Note that an OCM term is present in the update law for $\hat{\sigma}_p(t)$, but not for $\hat{\sigma}_q(t)$. In the initial design, it was not clear whether OCM was necessary in the calculation of the disturbance adaptive parameters. In the interest of keeping the controller as simple as possible, OCM was not included in either. During the first research flight, a persistent 1 Hz, ±0.5 deg/s oscillation was present in roll rate and was also observed in the value of $\hat{\sigma}_p(t)$. Implementation of OCM in that parameter's update law eliminated the oscillation on all of the remaining flights. Because a similar oscillation was not observed in $\hat{\sigma}_q(t)$, no OCM term was added for that parameter. During handling qualities maneuvers at the end of the flight phase of the experiment, interactions between the pilot and the pitch axis onMRAC+ controller were observed that likely adversely affected the pilot's rating of the system (refs. 13, 15). Subsequent simulation studies indicated that the addition of an OCM term to the $\hat{\sigma}_q(t)$ update law would eliminate these interactions.

Summary

Three model reference adaptive controllers, each representing an incremental increase in complexity, were designed and implemented as augmentation systems to a nonlinear dynamic inversion controller on a NASA F-18 test aircraft. The controllers were part of an experiment intended to evaluate the effect of adaptive controller complexity on performance, robustness, and pilot handling qualities in the event of aircraft failures or damage. The simplest controller is derived from basic MRAC theory and contains essentially a single adaptive parameter each in the pitch and roll axes. The more complex controllers expand upon the update laws and add a second adaptive parameter in each axis. Special design modifications are described to address biased measurements and other considerations required for implementation on a full-scale, piloted aircraft. Flight test results for the controllers are described in references 13 and 15.

Appendix A
Calculation of the P_q Matrix

The Lyapunov equation is given in equation (A1).

$$A_{m_q}^T P_q + P_q A_{m_q} = -Q_q \tag{A1}$$

For a second-order system in the form of equation (12) and a diagonal Q matrix, the Lyapunov equation is written as follows.

$$\begin{bmatrix} 0 & -\omega_q^2 \\ 1 & -2\zeta_q\omega_q \end{bmatrix}\begin{bmatrix} p_q^{11} & p_q^{12} \\ p_q^{21} & p_q^{22} \end{bmatrix} + \begin{bmatrix} p_q^{11} & p_q^{12} \\ p_q^{21} & p_q^{22} \end{bmatrix}\begin{bmatrix} 0 & 1 \\ -\omega_q^2 & -2\zeta_q\omega_q \end{bmatrix} = \begin{bmatrix} -q_q^{11} & 0 \\ 0 & -q_q^{22} \end{bmatrix} \tag{A2}$$

Expanding equation (A2) gives four equations with the four unknowns p_q^{mn}.

$$-\omega_q^2\left(p_q^{12} + p_q^{21}\right) = -q_q^{11} \tag{A3a}$$

$$p_q^{11} - \omega_q^2 p_q^{22} - 2\zeta_q\omega_q p_q^{12} = 0 \tag{A3b}$$

$$p_q^{11} - \omega_q^2 p_q^{22} - 2\zeta_q\omega_q p_q^{21} = 0 \tag{A3c}$$

$$p_q^{12} + p_q^{21} - 4\zeta_q\omega_q p_q^{22} = -q_q^{22} \tag{A3d}$$

It is clear from equations (A3b) and (A3c) that $p_q^{12} = p_q^{21}$, making the P_q matrix symmetric. From equation (A3a), the off-diagonal terms can be determined.

$$p_q^{12} = p_q^{21} = q_q^{11}\left(\frac{1}{2\omega_q^2}\right) \tag{A4}$$

Substitution of equation (A4) into equation (A3d) gives the expression for p_q^{22}.

$$p_q^{22} = q_q^{11}\left(\frac{1}{\omega_q^2}\right)\left(\frac{1}{4\zeta_q\omega_q}\right) + q_q^{22}\left(\frac{1}{4\zeta_q\omega_q}\right) \tag{A5}$$

Finally, equations (A4) and (A5) can be inserted into equation (A3b) or (A3c) to find p_q^{11} .

$$p_q^{11} = q_q^{11}\left(\frac{1 + 4\zeta_q^2}{4\zeta_q\omega_q}\right) + q_q^{22}\left(\frac{\omega_q}{4\zeta_q}\right) \tag{A6}$$

References

1. Whitaker, H. P., "Massachusetts Institute of Technology Presentation," *Proceedings of the Self Adaptive Flight Control Systems Symposium*, Wright Air Development Center, January 13-14, 1959, pp. 58-78.

2. Schuck, H. O., "Honeywell's History and Philosophy in the Adaptive Control Field," *Proceedings of the Self Adaptive Flight Control Systems Symposium*, Wright Air Development Center, January 13-14, 1959, pp. 123-145.

3. NASA Flight Research Center Staff, "Experience with the X-15 Adaptive Flight Control System," NASA TN D-6208, 1971.

4. Thompson, Milton O., and James R. Welsh, "Flight Test Experience with Adaptive Control Systems," Advanced Control System Concepts, AGARD CP No. 58, *AGARD Joint Symposium of the Guidance and Control Panel, and the Flight Mechanics Panel of AGARD*, Oslo Norway, September 3-5, 1968, pp. 141-147, 1970.

5. Monaco, J., D. Ward, R. Barron, and R. Bird, "Implementation and Flight Test Assessment of an Adaptive, reconfigurable Flight Control System," AIAA 97-3738, 1997.

6. Bosworth, John T., and Peggy S. Williams-Hayes, "Stabilator Failure Adaptation from Flight Tests of NF-15B Intelligent Flight Control System," *Journal of Aerospace Computing, Information, and Communication*, Vol. 6, March, 2009, pp. 187-206.

7. Burken, John J., Curtis E. Hanson, James A. Lee, and John T. Kaneshige, "Flight Test Comparison of Different Adaptive Augmentations to Fault Tolerant Control Laws for a Modified F-15 Aircraft," AIAA 2009-2056, 2009.

8. Krishnakumar, Kalmanje, "A Request for Information in Flight Validation of Adaptive Control to Prevent Loss-of-Control Events," Solicitation Number: NNH09ZEA002L, NASA Headquarters Office of Procurement, April 2009.

9. Greenwood, Donald T., *Principles of Dynamics*, Prentice Hall Inc., Upper Saddle River, New Jersey, 1988.

10. Miller, Christopher J., "Nonlinear Dynamic Inversion Baseline Control Law: Architecture and Performance Predictions," AIAA 2011-6467, 2011.

11. Ioannou, Petros A., and Jing Sun, *Robust Adaptive Control*, Prentice Hall Inc., Upper Saddle River, New Jersey, 1996.

12. McRuer, Duane., Irving Ashkenas, and Dunstan Graham, *Aircraft Dynamics and Automatic Control*, Princeton University Press, Princeton, New Jersey, 1973.

13. Hanson, Curt, Jacob Schaefer, John J. Burken, Marcus Johnson, and Nhan Nguyen, "Handling Qualities Evaluations of Low Complexity Model Reference Adaptive Controllers for Reduced Pitch and Roll Damping Scenarios," AIAA 2011-6607, 2011.

14. Nguyen, Nhan T., "Asymptotic Linearity of Optimal Control Modification Adaptive Law with Analytical Stability Margins," AIAA 2010-3301, 2010.

15. Schaefer, Jacob, Curt Hanson, Marcus A. Johnson, and Nhan Nguyen, "Handling Qualities of Model Reference Adaptive Controllers with Varying Complexity for Pitch-Roll Coupled Failures," AIAA 2011-6453, 2011.